Structural Monitoring and Maintenance, *Vol. 12, No. 1 (2025) 33-50*
https://doi.org/10.12989/smm.2025.12.1.033

Seismic performance of prestressing precast bridge columns with socket connection

Chongbin Zhang[1a], Shuang Zou*[2,3] and Heisha Wenliuhan[2,3b]

[1]*China Railway Engineering Design and Consulting Group Co., Ltd., Beijing, China*
[2]*Earthquake Engineering Research & Test Center, Guangzhou University, Guangzhou, Guangdong, China*
[3]*Key laboratory of Earthquake Engineering and Applied Technology in Guangdong Province, Guangzhou, China*

(*Received September 15, 2024, Revised October 15, 2024, Accepted October 18, 2024*)

Abstract. In order to fully utilize the advantages of large construction tolerance of socket connection and self-recovery of prestressed connection after earthquakes, a hybrid connection prefabricated assembled bridge pier (PCSC) with socket connection and prestressed reinforcement connection is proposed. Based on the actual engineering bridge pier, a finite element model of the pier was established using a fiber model, and the accuracy of the numerical model was verified by the in-situ full-scale test results. The performance indicators such as damage failure mode, hysteresis behavior, skeleton curve, energy dissipation capacity, equivalent stiffness, and residual displacement of the hybrid connected bridge pier was Analyzed. The results indicate that the failure mode of the PCSC bridge pier specimen is bending failure. The numerical analysis model established in this study can reproduce the experimental results well. The load displacement curve of PCSC bridge piers is roughly trilinear, and there is still a certain strengthening stage after yielding, with nonlinear inflection points and strength decline points. Compared with traditional cast-in-place (CIP) bridge pier, the configuration of unbonded post tensioned prestressed tendons in reinforced concrete hollow bridge piers greatly compensates for the weakened peak load and post yield stiffness of the piers due to the presence of connection, prolongs their yield point, improves ductility, yield strength, and horizontal resistance. The PCSC bridge piers exhibit weaker energy dissipation capacity. The prestressed tendons reduce the equivalent damping ratio of the bridge pier, increases the equivalent stiffness of the bridge pier, and has little effect on the residual displacement of the bridge pier.

Keywords: fiber model; in situ full-scale test; prefabricated connection; segmental bridge piers; socket connection

1. Introduction

In order to improve on-site construction efficiency and component quality, prefabricated assembly systems are becoming increasingly popular, and precast segmental concrete columns are one of them (Li *et al.* 2018, Zhang *et al.* 2021, Haraldsson *et al.* 2013, Li *et al.* 2016). Compared

*Corresponding author, Ph.D., E-mail: zoushuang_2015@163.com
[a]Ph.D., E-mail: zcb2002@163.com
[b]Professor, E-mail: wen.liuhan@a-sys.co.jp

http://www.techno-press.org/?journal=smm&subpage=7 ISSN: 2288-6605 (Print), 2288-6613 (Online)

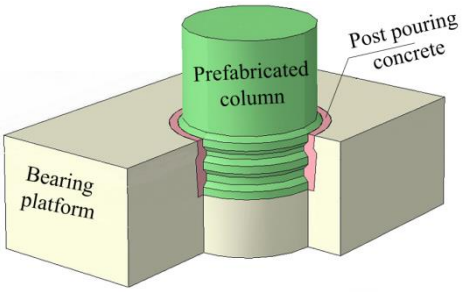

Fig. 1 SC bridge pier

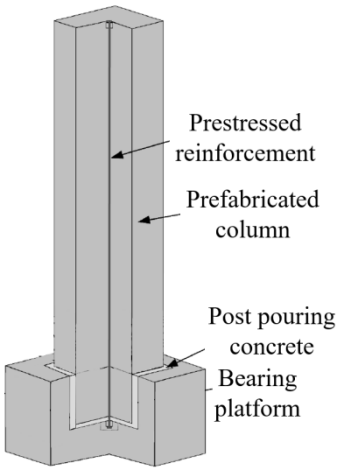

Fig. 2 PC bridge pier

with traditional cast-in-place (CIP) bridge piers, prefabricated segmental bridge piers have many advantages (Nikbakht *et al.* 2022). They can shorten on-site construction time and save construction period. Factory prefabricated pier and column segments can help improve the quality of piers, reduce the impact of construction on sensitive areas under the bridge and surrounding environment, reduce traffic interference in busy areas at the bridge site, and ensure the safety of construction workers in high-risk areas such as high altitude, sea, and highways, and reduce the full life cost of bridges, etc. (Wang *et al.* 2019, Tong *et al.* 2020, Sung *et al.* 2017).

At present, the prefabricated segmental bridge piers that are widely studied and applied mainly include prestressed connections, socket connections, grouted sleeve connections, and grouted corrugated pipe connections (Zou *et al.* 2022). Among them, socket connection refers to reserving slots larger than the size of the pier column in the socket, lifting the prefabricated pier column into the reserved hole, and pouring grouting material into the gap between the pier column and the reserved hole to make it a whole (Fig. 1) (Jin *et al.* 2011, Han *et al.* 2023, Wang *et al.* 2019). The socket connection (SC) bridge pier has advantages such as simple construction technology, fast construction speed, and large allowable errors, so it is widely used [12-13]. Previous research has shown that socket depth is a key parameter for socket connection. When the depth of the socket connection is not less than 1.0D, the design goal of "equivalent cast-in-place integral pier" SC

bridge pier can be achieved (Kan *et al.* 2003, Hieber *et al.* 2005). However, in order to ensure smooth railway traffic, railway bridge piers often need to have greater stiffness to reduce the displacement of the upper structure of the bridge during earthquakes. This makes most high-speed railway bridge pier columns designed with large cross-sectional dimensions and high stiffness. If the SC bridge pier column is designed according to the requirement of a socket depth of no less than 1.0D, it will inevitably greatly increase the thickness of the bearing platform, increase costs, and also bring about the problem of hydration heat during the pouring of large volume concrete (Zou *et al.* 2023). In addition, there is a problem of large residual displacement after earthquakes for SC bridge piers (Zou *et al.* 2023, Han *et al.* 2023).

Prestressed concrete (PC) bridge pier columns are decomposed into several lightweight components, which are prefabricated in the prefabrication yard and then transported to the construction site to be assembled into bridge pier columns (Bu *et al.* 2012). Then insert prestressed tendons into the reserved hole. Prefabricated components are assembled into integral bridge piers through the pre-pressure of prestressed tendons (Fig. 2) (Bao *et al.* 2023). Prestressed connections can significantly improve the self- recovery ability of bridge pier columns, but the connection method has poor energy dissipation ability, usually requiring additional dampers to dissipate seismic energy, and the column base in the compression zone is prone to damage (Wang *et al.* 2019).

In order to increase the energy dissipation capacity of PC bridge pier columns, Mohebb *et al.* (2018). arranged prestressed tendons on the basis of socket connections. The results showed that pre-stressing can significantly increase the self-resetting ability of prefabricated bridge pier columns. Therefore, fully utilize the advantages of the tolerance of the socket connection construction and achieve post-earthquake self-resetting of pier columns, and improve the energy consumption capacity of bridge piers, PC bridge columns with socket connection (PCSC) have been proposed.

In summary, this article combines the Hetian-Ruoqiang Railway Bridge Project to conduct on-site full-scale in-situ loading tests on PCSC. Based on the experiments, fiber model is established to explore the mechanical properties of prestressing precast bridge columns with socket connection. At the same time, the local damage, hysteresis curve, skeleton curve, cumulative energy consumption and other behaviors of the pier columns are compared and analyzed to verify the feasibility of the numerical modeling method. The research conducted on this basis will provide reliable basic research data for the promotion and application of PCSC bridge piers in China.

2. Research object

The PCSC bridge columns in the Hetan-Ruoqiang railway line were taken as the research object. As shown in Fig. 3, the PCSC bridge pier is a double column circular hollow section bridge pier, with a pier height of 12 m, an outer diameter of 1.8 m, a wall thickness of 0.4 m, and a lateral center distance of 2.8 m. The horizontal width of the pier cap beam is 5.6 m, the vertical width is 2.4 m, and the height is 1.3m. The lateral width of the pier bearing platform is 5.8 m, the longitudinal span is 5.8 m, and the height is 2.0 m.

The pier column is a single segment. The cap beam, piers column and bearing platform are connected by 6 prestressed tendons. The prestressed tendons are wrapped in a polyethylene pipe and passes through the interior of the concrete, with the lower part anchored at the bottom of the bearing platform. Place the pier columns inside the reserved connection foundation pit inside the

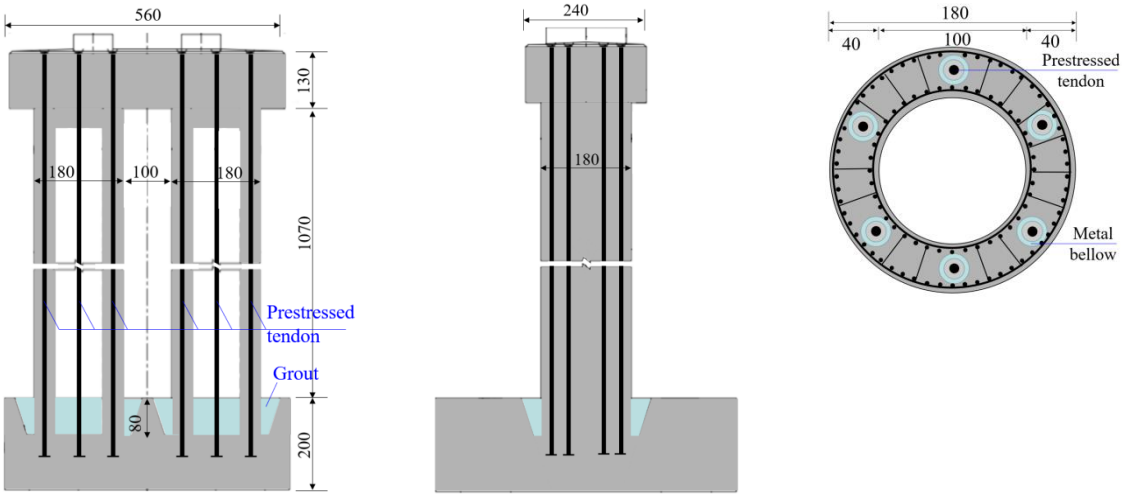

(a) (b) (c)

Fig. 3 PCSC bridge piers (cm)

Fig. 4 ZSM self-anchoring anchoring system

Table 1 The characteristic parameters of PCSC bridge piers

Material		Characteristic parameters
Prestressed tendons	Size	12Φ15.2 mm
	Yield strength	1890 (MPa)
	Initial stress	1116 (MPa)
Longitudinal reinforcement	Size	90D12
	Yield strength	410 (MPa)
Stirrup	Size	D12 @100 (Encrypted area); D12 @150
	Yield strength	410 (MPa)
Concrete	Yield strength	50 MPa

bearing platform, and after positioning are completed, tensions the prestressed tendons. The upper part of the prestressed tendons are anchored at the top of the cap beam. Apply epoxy adhesive between the cap beams, piers columns and bearing platform. Pour concrete into the reserved

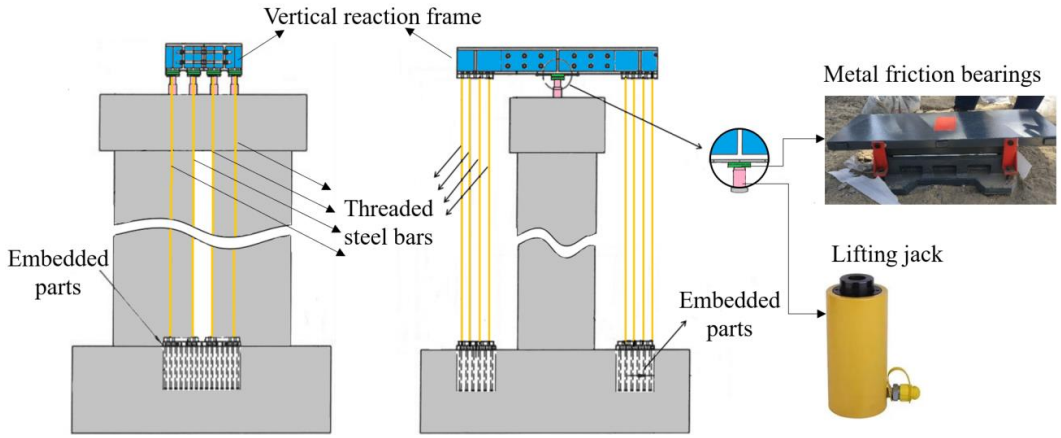

Fig. 5 Schematic diagram of vertical reaction frame

foundation pit of the pier bearing platform. Grouting between prestressed tendons and polyethylene sleeves to prevent corrosion of steel tendons and complete the overall connection of bridge piers. The longitudinal reinforcements are discontinuous at the connection of the each segment. As shown in Fig. 2, each pier column section is equipped with 6 prestressed tendons, each consisting of 12 Φ 15.2 mm high-strength low relaxation steel strands with a standard tensile strength of f_{pk}=1860 Mpa. The anchor adopts a matching ZSM self-anchoring anchoring system (Fig. 4). The tension control stress under the anchor is 1116 Mpa. The pier and abutments are made of concrete with a strength grade of C40, while other parts are made of concrete with a strength grade of C50. The reinforcement form of the pier column are shown in the figure, all using HRB400 hot-rolled ribbed steel bars with a diameter of 12 mm.

3. In situ full-scale load test

3.1 Test piece weighting

A constant vertical load of 200t is applied to the top of the cap beam by setting up a vertical reaction frame to simulate the actual dead load of the bridge pier. As shown in Fig. 5, the vertical reaction frame is anchored to the bearing platform by a loaded steel beam through 16 threaded steel bars with a diameter of 32 mm. Set a jack between the loading steel beam and the pier cap beam. By lifting the jack, an axial load is applied to the top of the cap beam in one go and remains constant throughout the entire experiment to simulate the constant load on the top of the bridge pier. At the same time, in order to reduce the constraint effect of vertical steel frames on the longitudinal displacement of bridge piers, the cylindrical steel bearings with very small friction coefficients were installed between the jack and the loading crossbeam. The maximum displacement of the bearing is 10 cm.

3.2 Loading system

Horizontal load is applied to the bridge pier cap beam through a horizontal reaction frame. The

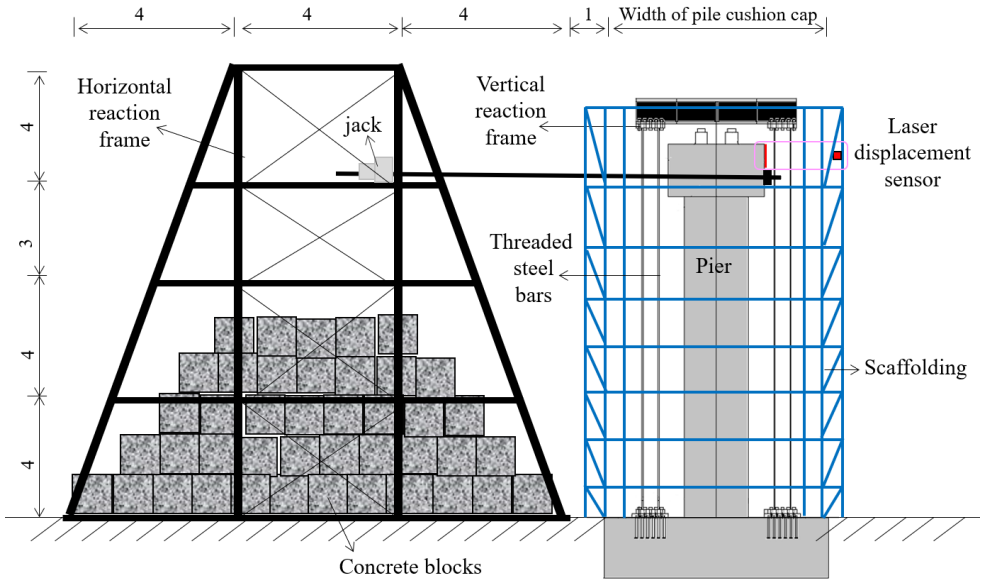

Fig. 6 Loading System

horizontal reaction frame, as shown in Fig. 6, is a highly rigid steel frame with a height of 15 m. Sufficient concrete blocks are stacked at the bottom of the horizontal reaction frame to ensure that the steel frame is not lifted when applying horizontal displacement loads to the bridge piers. Reserve a hole with a diameter of 15 cm at the center of the cap beam, anchor the prestressed tendons through one end of the cap beam, and connect the other end to a jack set at a height of 12 m above the ground on the horizontal reaction frame.

3.3 Test conditions

Apply horizontal displacement load step by step along the bridge using a jack, as shown in Fig. 7. Load control is displacement control. The loading displacement amplitudes are 5 mm, 10 mm, 15 mm, 20 mm, ... , 90 mm. Each level of load is held for 5 minutes, and observation and marking of damage phenomena are carried out.

3.4 Testing content

Install a laser displacement meter at the top of the bridge pier to measure the displacement at the top of the pier during horizontal loading. In order to observe the strain evolution process of concrete and steel bars in bridge pier specimens under horizontal loads, strain gauges were installed on the outer concrete and steel bars near the foot of column, plastic hinge area, and the height of the filled concrete. The arrangement of strain gauges is shown in Fig. 8.

3.5 Test results

3.5.1 Failure mode

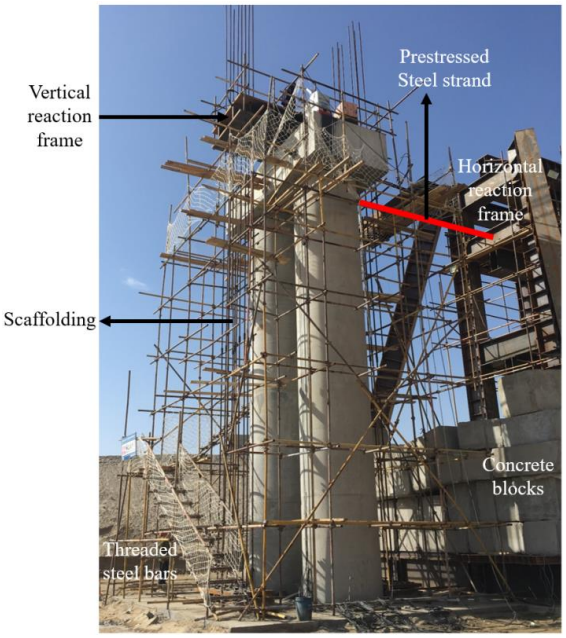

Fig. 7 Test loading site

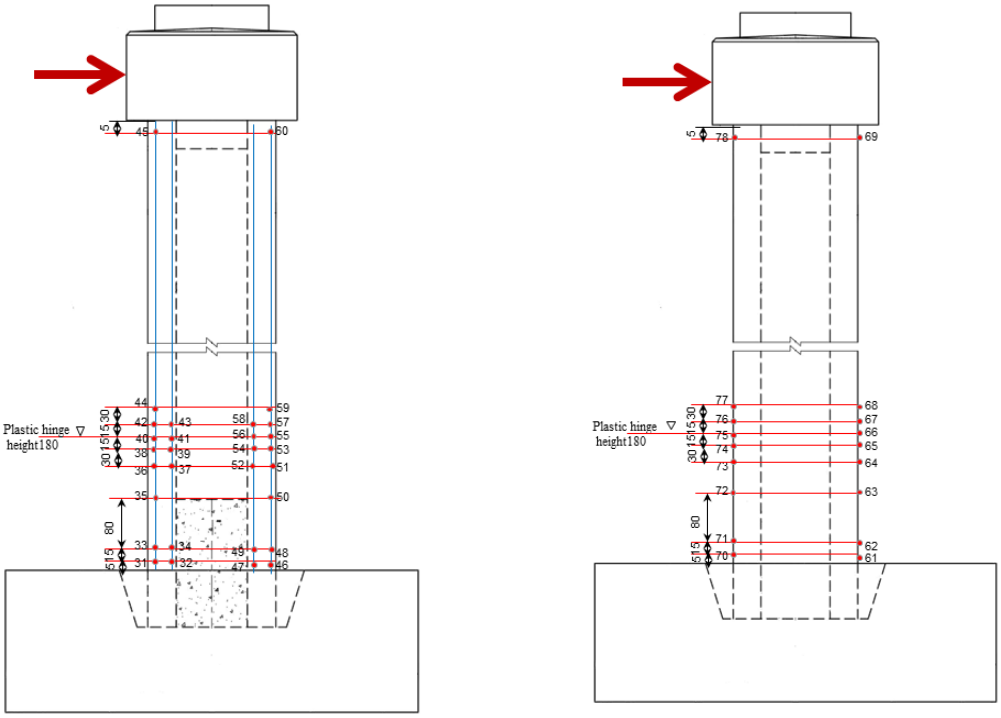

Fig. 8 Layout of strain measurement points (cm)

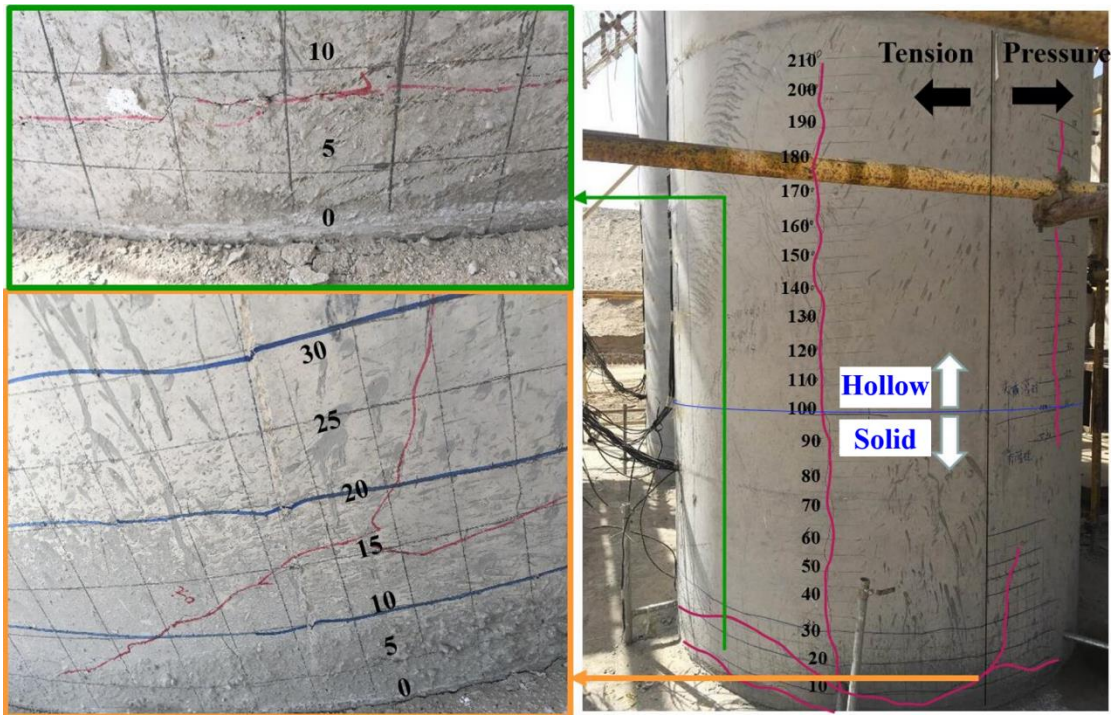

Fig. 9 Crack distribution diagram of the column specimen

The final state of PCSC bridge pier is shown in Fig. 9. The failure mode of the bridge pier specimen is bending failure, mainly manifested as slight cracking of the concrete protective layer at the root of the pier column. No plastic hinge occurred. This type of damage can be quickly repaired after a major earthquake. The Fig. 9 show that almost all cracks are mainly consisting of small cracks, and distributed on the surface of the connection area of pier column and the pier bearing platform. Due to the development of small cracks, it can effectively prevent damage to the plastic hinge area of the bridge pier.

3.5.2 Strain analysis

Table 2 shows the situation where the concrete and steel bars of the pier specimen reach the ultimate tensile strain measured by strain gauges under step-by-step displacement load loading.

As shown in the table, when the horizontal loading displacement at the top of the pier specimen reached 21 mm, the first crack was observed on the tensile side of pier column, located at the connection of the pier column and the bearing platform (Measurement point 70#). When the horizontal loading displacement reaches 31mm, the concrete at the bottom of the pier column (Measurement point 71#), the sudden stiffness change of the pier column (Measurement point 72#), and the plastic hinge height of the pier column (1800 mm) (Measurement point 73# and 74#) reaches the ultimate tensile strain and circumferential cracks appear. When the horizontal loading displacement reaches 40 mm, at the area of the plastic hinge, the strain of the concrete at more measuring points gradually reaches the ultimate tensile strain, indicating an intensification of concrete cracking in the plastic hinge area. The compressive strain of the concrete on the

Table 2 The measuring point enters the yielding state

Horizontal displacement （cm）	Measurement points reaching ultimate strain	
	Concrete	Reinforcement
21	$70^{\#}$	$31^{\#}$
31	$71^{\#}$、$72^{\#}$、$73^{\#}$、$74^{\#}$	—
40	$75^{\#}$、$76^{\#}$、$77^{\#}$	$32^{\#}$

compression side did not reach the ultimate compressive strain, and the concrete was in an unconfined state. No cracks were observed at the connection of the pier column top, and the concrete did not reach its ultimate tensile strain. This indicates that the concrete in the plastic hinge region is most prone to tensile failure.

When the horizontal loading displacement reaches 21 mm, the outer reinforcement at the bottom of the pier column reaches the ultimate tensile strain, and the outer reinforcement of the pier column begins to yield. When the horizontal loading displacement reaches 40 mm, the inner reinforcement at the bottom of the pier column reaches the ultimate tensile strain, and the inner reinforcement of the pier column begins to yield. The steel bars at other measuring points remain in an elastic state until the end of loading. This indicates that the reinforcements at the bottom of PCSC bridge pier are the first to fail.

4. Finite element analysis

In this paper, the fiber finite element model is used to verify the hysteretic capacity of the PCSC bridge pier and CIP bridge piers. As shown in Fig. 10, the fiber modeling techniques, based on software Uc-win/FRAME(3D), are schematically described. The top load on the top of the pier is simulated using a concentrated mass element. The bottom position of the pier bearing platform is consolidated.

The entire model includes 2 elastic beam elements and 20 elastic-plastic fiber beam column elements. The 2 elastic beam elements were used to simulate the bearing platform and cap beam. Using reinforced concrete fiber beam column elements to simulate the pier columns. The reinforced concrete section is discretized into core concrete fibers constrained by hoops, protective layer concrete fibers, and steel reinforcement fibers (Zhu *et al.* 2021, Fu *et al.* 2024). The constitutive relationship of concrete is simulated using the Mander model. The core constraint concrete is shown in Fig. 10(a). The steel reinforcement fibers are simulated using the Menegotto Pinto model. The prestressed tendons adopts an ideal elastic-plastic model, and its constitutive relationship curve is shown in Fig. 10(a). The plain concrete fiber beam column elements was used to simulate the mechanical properties of connection parts, as shown in element 1, element 2, element 11, element 12 and element 22 in Fig. 10(a). The top prestressed anchorage end of the prestressed tendon is connected to the top of the column with a rigid wall, and the bottom is consolidated with the bearing platform. The cross-sectional grid division of the pier columns fiber unit, as well as the arrangement of steel bars, concrete, and prestressed tendons, are shown in Fig. 8(a).

The model is loaded according to displacement based on the test loading system.

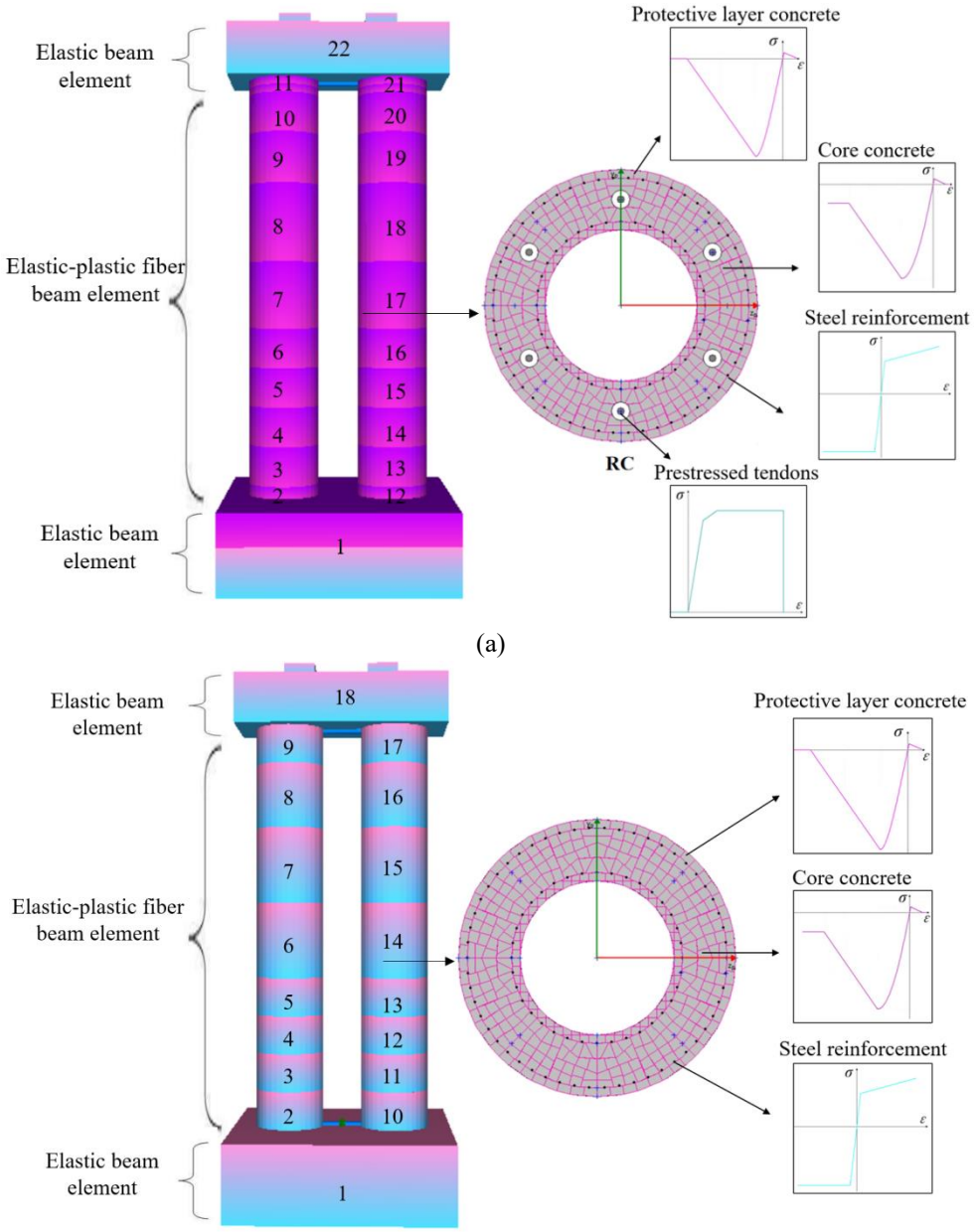

Fig. 10 Finite element model of pier column fiber

5. Analysis results

In order to compare and analyze, a cast-in-place (CIP) bridge pier with the same size and reinforcement as the bridge pier specimen was also established for quasi-static analysis.

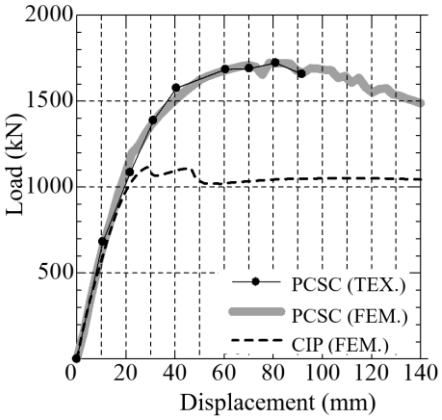

Fig. 11 Load-displacement curves

5.1 Load-displacement curves

The load-displacement relationship curves was shown in Fig. 11. Among them, the black solid line is the load-displacement relationship curve of the PCSC bridge pier specimen measured by the experiment. The gray thick line is the load-displacement relationship curve of PCSC bridge pier specimens obtained from numerical analysis. The black dashed line is the load - displacement relationship curve of the CIP bridge pier obtained from numerical analysis. The equivalent yield point and corresponding load values of the load-displacement curves are shown in Table 3. According to the load-displacement curves and the key points of strength deformation, it can be inferred that:

(1) Considering the safety of on-site full-scale testing and the limitations of testing equipment, the horizontal displacement load was only loaded to 90mm (0.8%) and did not reach the ultimate displacement of the pier specimen. And the load-displacement relationship curve of PCSC bridge pier connection is roughly trilinear, and after yielding, there is still a certain strengthening stage, with nonlinear inflection points and strength decline points.

(2) The load-displacement relationship curve of the PCSC bridge pier obtained from the fiber model analysis is in good agreement with the load-displacement relationship curve measured in the experiment. This indicates that the fiber finite element model established in this study can accurately simulate the mechanical properties of PCSC bridge piers.

(3) The shape of the load displacement curve of CIP concrete bridge pier is similar to a flag shaped curve. The bearing capacity of the bridge pier remains stable after yielding, without any significant strength decrease.

(4) Compared with CIP bridge pier, the elasticity of PCSC bridge pier has decreased by 10.6%, the yield load has increased by 60.8%, the maximum horizontal bearing capacity has increased by 54.4%, and the displacement ductility has decreased by 53.4%. This indicates that the use of prestressed tendons can effectively improve the ultimate bearing capacity of PCSC bridge piers. However, after the PCSC bridge piers reach their ultimate load, their bearing capacity rapidly decreases. After the CIP bridge piers yield, their bearing capacity remains unchanged without a significant downward trend, and their displacement ductility is significantly better than that of PCSC bridge piers.

Table 3 Strength and deformation key points

Case	First cracking		Yield		Maximum bearing capacity		Ultimate failure		displacement ductility
	Force (kN)	Displacement (mm)	Force (kN)	Displacement (mm)	Force (kN)	Displacement (mm)	Force (kN)	Displacement (mm)	
PCSC(TEX.)	1371	31.0	1497	38.7	1722	81.0	—	—	—
PCSC(FEM.)	1387	31.2	1504	37.0	1722	81.0	1483	126.0	4.04
CIP(FEM.)	947	19.0	1045	23.0	1115	29.0	1020	165.0	8.68

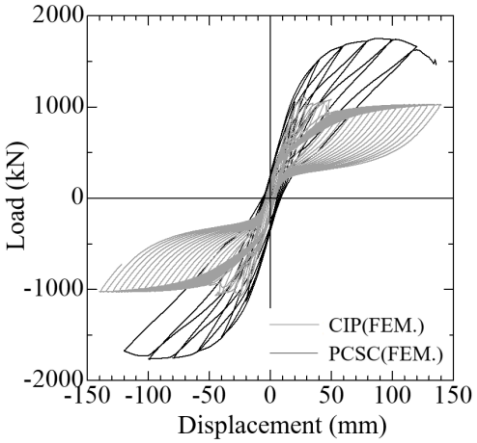

Fig. 12 Hysteresis curves

5.2 Hysteresis curves

The hysteresis curves of CIP bridge piers and PCSC bridge piers obtained from fiber model analysis are shown in Fig. 12. From the comparative analysis of hysteresis loops, it can be seen that in the small load stage, the two type bridge piers are basically in the elastic stage, and the hysteresis loops are concentrated and overlapped. With the occurrence of phenomena such as cracking of concrete, yielding of ordinary steel bars, and the development of cracks, the hysteresis loops gradually opens up and presents a shuttle shape, increasing the area enclosed by the hysteresis loops and enhancing energy dissipation. During this stage, the hysteresis curves of the CIP bridge pier exhibited a significant pinching effect, with the hysteresis curves taking on a "flag" shape. The PCSC bridge pier, due to the sufficient restoring force provided by the prestressed tendons, still has no significant hysteresis curve pinching effect until the pier reaches its ultimate displacement.

5.2.1 Energy consumption capacity

Fig. 13 shows the energy dissipation capacity curves of CIP bridge pier and PCSC bridge pier under six different peak displacement hysteresis loops analyzed using a fiber model. As shown in the figure, with the increase of loading displacement, the energy dissipation capacity of the bridge pier increases. When the horizontal displacement of the pier top is 120 mm, the energy

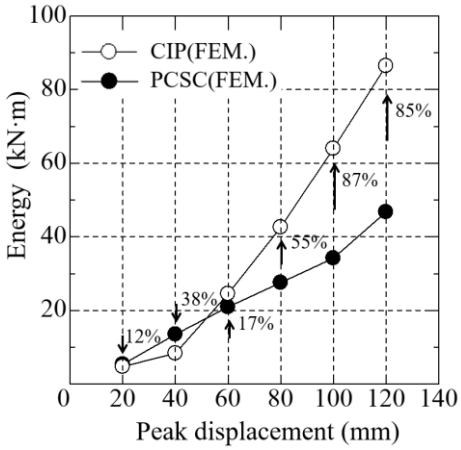

Fig. 13 Energy consumption capacity curves

consumption of the CIP bridge pier is 85% higher than that of the PCSC bridge pier. This indicates that compared to CIP bridge piers, PCSC bridge piers have weaker energy dissipation capacity.

5.2.2 Equivalent stiffness and equivalent viscous damping ratio

According to Priestley *et al.* (Sung *et al*. 2017), the equivalent viscous damping ratio is defined as follows

$$\xi_{eq} = \frac{A_h}{2\pi V_m \Delta_m} = \frac{A_h}{4\pi A_e} \tag{1}$$

$$k_{eff} = \frac{V_m}{\Delta_m} \tag{2}$$

$$\text{Where} \quad F_m = \frac{|V_{\max}| + |V_{\min}|}{2} \tag{3}$$

$$\Delta_m = \frac{|\Delta_{\max}| + |\Delta_{\min}|}{2} \tag{4}$$

In the formula, ξ_{eq} is the equivalent viscous damping ratio; A_h is the area of a complete force-displacement hysteresis loop, i.e., dissipated energy; V_m and Δ_m are the average maximum load and average maximum displacement; K_{eff} is the effective stiffness of an equivalent linear elastic system; A_e is the elastic strain energy. V_{max} and V_{min} are the maximum positive and negative horizontal loads at a certain displacement, respectively; Δ_{max} and Δ_{min} are the maximum positive and negative displacement, respectively.

Fig. 14 shows the equivalent viscous damping ratio curves of PCSC bridge piers and CIP bridge piers obtained through fiber model analysis. As shown in the figure, as the loading progresses, the equivalent viscous damping ratio of the PCSC bridge pier tends to stabilize, maintaining around 0.35. The initial equivalent damping ratio of CIP bridge piers is basically the same as the PCSC bridge piers. When the horizontal displacement load reaches 40mm, the CIP

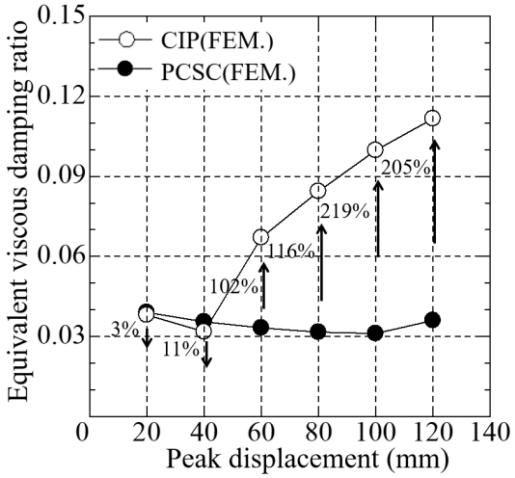

Fig. 14 Equivalent viscous damping ratio curves

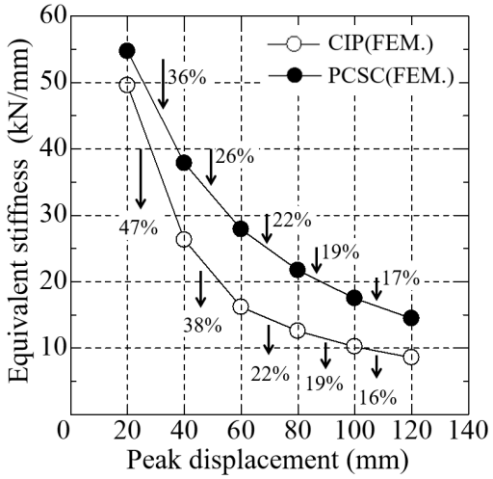

Fig. 15 The equivalent stiffness

bridge pier enters the plastic stage. While the horizontal force remains unchanged, the horizontal displacement continues to increase, and the equivalent viscous damping ratio of the CIP bridge pier significantly increases. When the horizontal load at the top of the pier is 120 mm, the equivalent viscous damping ratio of the PCSC bridge pier is reduced by 67.2% compared to the CIP bridge pier.

Fig. 15 shows the equivalent stiffness curves of PCSC bridge piers and CIP bridge piers obtained through fiber model analysis. As shown in the figure, with the increase of loading displacement, the equivalent stiffness of both PCSC bridge piers and CIP bridge pier shown a decreasing trend. Due to the use of prestressed tendons, the equivalent stiffness of PCSC bridge pier is higher than CIP bridge pier. When the horizontal load at the top of the pier is 120 mm, the equivalent stiffness of the PCSC bridge pier is increased by 66.7% compared to the CIP bridge pier.

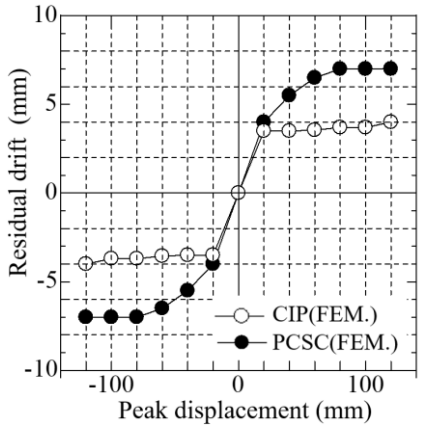

Fig. 16 Residual displacement curves

Especially when the horizontal displacement load is less than 60mm, the decrease in equivalent stiffness of CIP bridge pier is significantly greater than PCSC bridge pier. When the horizontal displacement load exceeds 60mm, the equivalent stiffness of the two types of bridge piers decreases at the same rate. This is because prestressed tendons not only improve the bearing capacity of PCSC bridge pier, but also increase the equivalent stiffness of PCSC bridge pier. The displacement is small, and the effect of prestressed steel bars is significant. As the displacement at the top of the pier increases and the prestressed tendons fail, PCSC piers and CIP piers exhibit the same equivalent stiffness.

5.2.3 Residual displacement

The average residual displacement in a single cycle was considered as the residual displacement of the bridge pier under six levels of hysteresis displacement. The relationship between the residual displacement of the loading displacement for PC bridge piers and CIP bridge pier are shown in Fig. 16. As shown in the figure, before the horizontal displacement reaches 0.2%, the residual displacement of the PC bridge piers and CIP bridge is basically the same, indicating that under the restoring force of prestressed tendons, these two forms of bridge piers exhibit similar hysteresis performance. However, after the horizontal displacement exceeded 0.2%, significant behavioral differences were observed between the two forms of bridge piers. As the displacement load increases, the residual deformation of the CIP bridge pier remains unchanged after reaching a certain value. This result indicates that at this point, the concrete of the bridge pier has entered yield, and only the steel bars bear displacement loads, while the steel bars are in an elastic state and the residual displacement remains unchanged. When the horizontal displacement is within the range of 0.2% to 0.7%, the steel reinforcement of the PC bridge pier is in an elastic-plastic state. As the horizontal displacement load increases, the residual displacement also shows an increasing trend. After the horizontal displacement exceeds 0.7%, the precast prefabricated pier concrete also enters a yielding state, and the prestressed tendons bear the horizontal displacement load. Due to the elastic state of the prestressed tendons, the residual deformation at this stage is a fixed value. Comparing the residual deformation differences between PC bridge piers and CIP bridge piers, it can be seen that the use of prestressed steel strands has a relatively small impact on the residual displacement of the bridge piers, with a difference of only 3 mm.

6. Conclusions

Based on the Hetian-Ruoqiang Railway Bridge Project to conduct on-site full-scale in-situ loading tests on PCSC bridge pier. Through experiments and fiber model numerical simulation analysis, the mechanical properties of PCSC bridge pier are studied. The main conclusions are as follows.

(1) In full-scale tests, the failure mode of the PCSC bridge pier specimen is bending failure, mainly manifested as slight cracking of the concrete protective layer at the root of the pier column. No plastic hinge occurred.

(2) The load-displacement relationship curve of the PCSC bridge pier obtained from the fiber model analysis is in good agreement with the load-displacement relationship curve measured in the experiment. The fiber finite element model established in this study can accurately simulate the mechanical properties of PCSC bridge piers.

(3) The load displacement curve of PCSC bridge piers is roughly trilinear, and there is still a certain strengthening stage after yielding, with nonlinear inflection points and strength decline points. Compared with CIP bridge pier, the elasticity of PCSC bridge pier has decreased by 10.6%, the yield load has increased by 60.8%, the maximum horizontal bearing capacity has increased by 54.4%, and the displacement ductility has decreased by 53.4%. The configuration of unbonded post tensioned prestressed tendons in reinforced concrete hollow bridge piers greatly compensates for the weakened peak load and post yield stiffness of the piers due to the presence of connection, prolongs their yield point, improves ductility, yield strength, and horizontal resistance. the PCSC bridge piers exhibit weaker energy dissipation capacity.

(4) The prestressed tendons reduce the equivalent damping ratio of the bridge pier, increases the equivalent stiffness of the bridge pier, and has little effect on the residual displacement of the bridge pier. When the horizontal displacement of the pier top is 120 mm, compared with the CIP bridge pier, the equivalent damping ratio of the PCSC bridge pier decreases by 67.2%, the equivalent stiffness increases by 66.7%, and the residual displacement only increases by 3 mm.

Acknowledgments

This research was funded by the National Science Foundation of China (Grant Nos. 52308487), China Railway Research and Development Program Project (2024-Key-07), and Research and Development Plan Project of the China Railway Engineering Design Consulting Group (Research 2022-5 and Research 2023-5).

References

Bao, L.S., Zhao, J.K., Teng, F., Kong, Z., Yu, L., Bao, Y.Y., Zhao, T.F. and Yang, Y.H. (2023), "Experimental study on the seismic performance of precast segmental unbonded post-tensioned frame piers", *Soil Dyn. Earthq. Eng.*, **173**, 108143. https://doi.org/10.1016/j.soildyn.2023.108143.

Bu, Z.Y., Ding, Y., Chen, J. and Li, Y.S. (2012), "Investigati. on of the seismic performance of precast segmental tall bridge columns", *Struct. Eng. Mech.*, **43**(3), 287-309. https://doi.org/10.12989/sem.2012.43.3.287.

Fu, X., Du, W.L., Li, G., Dong, Z.Q. and Li, H.N. (2014), "A data-driven method for the reliability analysis of a transmission line under wind loads", *Steel Compos. Struct.*, **52**(4), 461-473.

https://doi.org/10.12989/scs.2014.52.4.461.
Han, Y., Ding, S.C., Qin, Y.X. and Zhang, S.L. (2023), "Test for the influence of socket connection structure on the seismic performance of RC prefabricated bridge piers", *Earthq. Struct.*, **25**(2), 89-97. https://doi.org/10.12989/eas.2023.25.2.089
Han, Y., Huang, Z.M. and Li, Z.X. (2023), "Calculation of vehicle impact force on socket prefabricated Bridge Piers", *KSCE J. Civil Eng.*, **27**(10), 4362-4380. https://doi.org/10.1007/ s12205-023-2110-9.
Haraldsson, O.S., Janes, T.M., Eberhard M.O. and Stanton J.F. (2013), "Seismic resistance of socket connection between footing and precast column", *J. Bridge Eng.*, **18** (9), 910-919. https://doi.org/10.1061/(ASCE)BE.1943-5592.00004.
Hieber, D.G. and Wacker, J.M. (2005), "State-of the art report on precast concrete systems for rapid construction of bridges", Washington: Washington State Transportation Commission, Department of Transportation, WA-RD 594.
Jin, Z.B., Chen, K. and Pei, S.L. (2011), "Cyclic response of precast, hollow bridge columns with post pour section and socket connection", *J. Struct. Eng.*, **148**(1), 06021005. https://doi.org/10.1061/(ASCE)ST.1943-541X.0003220.
Kan, W.P. and Billington, S.L. (2003), "Unbonded posttensioned concrete bridge piers II: Seismic analyses", *Journal of Bridge Engineering*, **8**(2), 102-111. https://doi.org/10.1061/(ASCE)1084-0702(2003)8:2(102).
Li, C., Hao, H. and Bi, K.M. (2017), "Numerical study on the seismic performance of precast segmental concrete columns under cyclic loading", *Eng. Struct.*, **148**, 373-386. https://doi.org/10. 1016/j. engstruct. 2017.06.062.
Li, C., Hao, H., Zhang, X.H. and Bi, K.M. (2018), "Experimental study of precast segmental columns with unbonded tendons under cyclic loading", *Adv. Struct. Eng.*, **21**(3), 319-334. https://doi.org/10.1177/1369433217717119.
Li, Z.X., Yu, C. and Shi, Y.D. (2016), "Seismic damage control of nonlinear continuous reinforced concrete bridges under extreme earthquakes using MR dampers", *Soil Dyn. Earthq. Eng.*, **88**, 386-398. https://doi.org/10.1016/j.soildyn.2016.07.015.
Mohebbi, A., Saiidi, M.S. and Itani, A.M. (2018), "Shake table studies and analysis of a PT-UHPC bridge column with pocket connection", *J. Struct. Eng.*, **144**(4), 04018021. https://doi.org/10.1061/(ASCE)ST.1943-541X.0001997.
Nikbakht, E., Rashid, K., Mohseni, I. and Hejazi, F. (2015), "Evaluating seismic demands for segmental columns with low energy dissipation capacity", *Earthq. Struct.*, **8**(6), 1277-1297. https://doi.org/10.12989/eas.2015.8.6.1277
Si X.L., Wen J.N., Zhang G.D., Jia Z.L., Han Q. (2023), "Seismic performance of precast double-column pier with UHPC-filled socket connections", *Eng. Struct.*, **285**, 115618. https://doi.org/10.1016/j.engstruct.2023.115618.
Sung, Y.C., Hung, H.H., Lin, K.C. and Jiang, C. (2017), "Experimental testing and numerical simulation of precast segmental bridge piers constructed with a modular methodology", *J. Bridge Eng.*, **22**(11), 04017087. https://doi.org/10.1061/(ASCE)BE.1943-5592.0001122.
Tong, T., Zhou, W.D., Jiang, X.F., Lei, H.P. and Liu, Z. (2020), "Research on seismic resilience of prestressed precast segmental bridge piers reinforced with high-strength bars through experimental testing and numerical modelling", *Eng. Struct.*, **197**, 109335. https://doi.org/10.1016/j.engstruct. 2019.109335.
Wang, J.Q.， Wang, Z., Gao, Y.F. and Zhu, J.Z. (2019), "Review on aseismic behavior of precast piers: new material, new concept, and new application", *Eng. Mech*., **36**(3), 1-23. (In Chinese)
Wang, Z.Q., Li, T.T., Qu, H.Y., Wei, H.Y. and Li, Y.B. (2019), "Seismic performance of precast bridge columns with socket and pocket connections based on quasi-static cyclic tests: experimental and numerical study", *J. Bridge Eng.*, **24**(11), 04019105. https://doi.org/10.1061/(ASCE)BE.1943-5592.0001463.
Zhang, G.D., Han, Q., Xu, K., Du, X.L. and He, W.L. (2021), "Quasi-static tests of CFST embedded RC column-to-precast cap beam with shallow socket connection", *Eng. Struct.*, **241**, 112443. https://doi.org/10.1016/j.engstruct.2021.112443.

Zhang, Y.G., Chen, L., Zuo, R., Xie, H.H., Yang, S.W., Zhang, K.F. and Hu, Z.L. (2023), "Experimental and numerical study of precast bridge piers with a new UHPC socket column-footing connection", *Archiv. Civil Mech. Eng.*, **24**(1), 17. https://doi.org/10.1007/s43452-023-00829-x.

Zhu, L.H., Li, G. and Dong, Z.Q. (2021), "Dynamic test and numerical simulation on avoiding the weak-story failure mechanism in structures using LSFDs", *Steel Compos. Struct.*, **40**(2), 175-191. https://doi.org/10.12989/sem.2021.40.2.175.

Zou, S., Wenliuhan, H.S., Liu, Y.H., Zhai, Z.P. and Zhang, C.B. (2023), "Seismic performance of precast assembled bridge piers with hybrid connection", *Struct. Eng. Mech.*, **85**(3), 407-417. https://doi.org/10.12989/sem.2023.85.3.407.

Zou, S., Wenliuhan, H.S., Mao, Y.P., Yu, B.P. and Zhang, C.B. (2020), "Cyclic test and numerical study of seismic performance of precast segmental concrete double-columns", *J. Central South Univ.*, **29**, 2502-2512. https://doi.org/10.1007/s11771-022-5092-8.

Zou, S., Zhang, C.B., Wenliuhan, H.S., Yang, Z.Y., Liu, Y.H., Zhai, Z.P. and Feng, H. (2023), "Seismic performance of precast hollow concrete bridge double columns with shallow socket connection", *Soil Dyn. Earthq. Eng.*, **171**, 107957.